

Study on Brake Control for High-Speed Train Based on Optimal Distribution of Braking Force

Jing He¹, Pengjuan Zhao¹, Changfan Zhang¹, Jianhua Liu²

¹(College of Electrical and Information Engineering, Hunan University of Technology, Hunan, Zhuzhou 412007, China)

²(College of Traffic Engineering, Hunan University of Technology, Hunan, Zhuzhou 412007, China)

ABSTRACT : To solve the problem of train sliding caused by unreasonable braking force distribution in high-speed train braking process, it presented a vehicle braking force distribution algorithm in the paper. Firstly, a high-speed train dynamic model of the coupling force between trains and running resistance was established. Secondly, a sliding mode controller was designed to solve the longitudinal target braking force of the train. Finally, quadratic programming was adopted to solve the objective function further by establishing the objective optimization function using adhesion utilization, taking the two constraints (i.e., adhesion limit and passenger ride comfort) into consideration. It could be concluded based on the results of the simulation experiment that, the optimized control algorithm in this paper could ensure that each car was running well after the braking force was distributed.

KEYWORDS: high-speed train, sliding mode control, optimized braking force distribution, adhesion limit, ride comfort.

Date of Submission: 05-02-2021

Date of Acceptance: 18-02-2021

I. INTRODUCTION

A high-speed train is provided with braking force by its several carriages. The effective exertion of the braking force depends on the adhesive force formed when the wheel comes in contact with the rail [1]. In practice, the braking force exerted by a high-speed train should be less than the designed maximum adhesive force between the wheel and the rail; otherwise, the train will slide [2]. If the train slides, it will lead to a loss of braking force, further resulting in cascading failures, and the train may even be forced to stop [3]. As the braking state of each carriage is different, the braking force borne by each carriage also varies. Therefore, the research on a reasonable and effective braking force distribution strategy is of great significance to improve the braking efficiency, shorten the braking time, and ensure the safe operation of high-speed trains [4].

With the aim of solving the problems regarding high-speed train braking force distribution, experts at home and abroad have conducted a variety of research. Zhu et al. (2013) [5] used electro-pneumatic braking priority control principle in Electric Multiple Unit, and distributed the air braking force required by the trailer and the motor car based on the inverse ratio of the load. An optimized control strategy was proposed to further effectively reduce the wear of the trailer wheel and brake shoe. On the basis of the requirement of tramcars to ensure traction/braking force in different operation states, Li et al. (2020) [6] proposed a braking force distribution method in which the electric braking is the prior condition and combined the mechanical characteristic curve of traction motor. To solve the problem related to the short driving distance of electric vehicles, Ma ZW et al. (2020) [7] proposed a braking energy recovery strategy based on the ideal distribution of braking force. Besides ensuring both braking efficiency and braking stability, a braking energy recovery system was proposed to effectively realize the autonomous braking function under different braking conditions. Zhu et al. (2020) [8] proposed a multi-target optimized regenerative braking control strategy to improve the braking performance and regenerated energy of electric vehicles. This strategy could effectively improve the braking comfort and battery life without reducing the recovery energy. This strategy could effectively improve the braking comfort and battery life without reducing the recovery energy. In the abovementioned studies on the distribution of braking force, the main focus was on the theoretical control strategy. However, no in-depth study has been conducted on the weight of each carriage in the whole train, the adhesion restriction of each carriage, and the ride quality of passengers.

Aiming to solve the abovementioned problems, He et al. (2018) [9] proposed an optimal allocation algorithm of air braking force by taking the maximum value of total adhesion utilization as the objective function and the adhesion restriction as the constraint condition. The simulation result showed that their algorithm was superior to the traditional load ratio allocation algorithm. However, after a high-speed train is run safely and reliably and parked within a specified distance, the comfort of passengers should also be ensured [10].

In the existing research, longitudinal acceleration is usually used as the key index to evaluate ride comfort. To comprehensively measure the comfort of passengers, Ma HR et al. (2020) [11] proposed a combined fuzzy set model in which the measured acceleration data were used to verify and optimize the proposed model. Their result showed that the model could provide an alternative method for the train control system to measure ride comfort. González et al. (2016) [12] proposed a new velocity curve generator to improve the comfort of automatic vehicles by restricting the overall acceleration in the whole driving process. Their result showed that the smoothness of the acceleration curve could be significantly improved. Therefore, adhesion restriction and ride comfort are the constraints to be simultaneously considered for a high-speed train braking system.

This study proposes an optimized distribution algorithm of vehicle braking force in consideration of adhesion restriction and ride comfort. The contributions of the optimized distribution method in terms of research value are as follows: 1) In calculating target braking force that considers the interactive force between carriages, the multi-particle model used in this study is close to the actual situation as a means of describing the dynamic behavior of a train. 2) In the process of braking force distribution, the constraint conditions selected in this study take both the adhesion restriction and ride comfort of passengers into account. Longitudinal acceleration is used to measure the ride comfort of passengers, and braking force is further limited by restricting the acceleration.

II. DYNAMIC MODEL OF HIGH-SPEED TRAIN

Assuming that a high-speed train has n carriages. one carriage of the high-speed train is taken as an example for dynamic analysis. The dynamic model of the high-speed train obtained in this research is shown in Fig. 1.

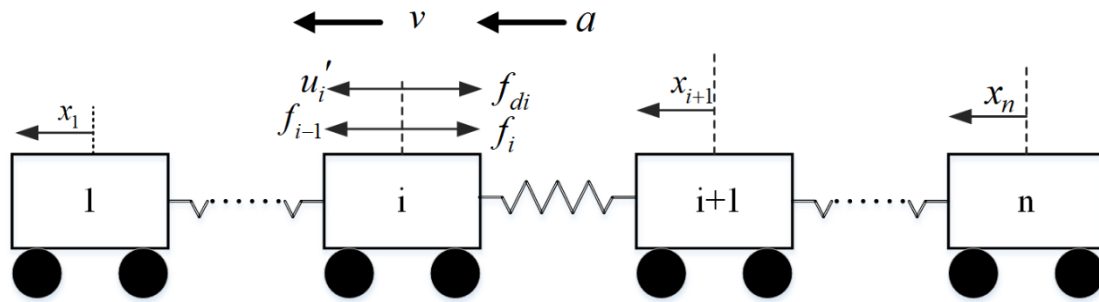


Fig. 1: Dynamic model of a high-speed train

On the basis of the force analysis of all of the carriages, the following dynamic equation can be obtained according to Newton's second law [13]:

$$\begin{pmatrix} m_1 & & & \\ & m_2 & & \\ & & \ddots & \\ & & & m_n \end{pmatrix} \begin{pmatrix} \ddot{x}_1 \\ \ddot{x}_2 \\ \vdots \\ \ddot{x}_n \end{pmatrix} = \begin{pmatrix} u'_1 \\ u'_2 \\ \vdots \\ u'_n \end{pmatrix} - \begin{pmatrix} f_{d1} \\ f_{d2} \\ \vdots \\ f_{dn} \end{pmatrix} + \begin{pmatrix} f_0 \\ f_1 \\ \vdots \\ f_{n-1} \end{pmatrix} - \begin{pmatrix} f_1 \\ f_2 \\ \vdots \\ f_n \end{pmatrix} \quad (1)$$

where $i = 1, 2, \dots, n$ refers to the number of carriages; m_i refers to the mass of the i_{th} carriage; x_i , \dot{x}_i and \ddot{x}_i refer to the displacement, velocity, and acceleration of the i_{th} carriage, respectively; u'_i refers to the control input of the i_{th} carriage; f_{di} refers to the running resistance on the i_{th} carriage; and f_i refers to the interactive force between the i_{th} carriage and the $(i+1)_{th}$ carriage.

The basic running resistance f_{di} of the train consists of two parts, the mechanical running resistance and the aerodynamic running resistance. The calculation equation of the basic resistance is given by [14]:

$$f_{di} = \varphi_1 + \varphi_2 v_i + \varphi_3 v_i^2 \quad (2)$$

where φ_1 , φ_2 and φ_3 are constants corresponding to the types of high-speed trains.

A high-speed train is a multi-body system, in which many carriages are connected in a physical coupling. The interactive force between carriages can be expressed as [15]:

$$f_i = k(x_i - x_{i+1}) + h(v_i - v_{i+1}) \quad (3)$$

where k refers to the coefficient of spring, and h refers to the coefficient of damping.

In selecting the state vector of the train, $\mathbf{X} = [x_1, x_2, \dots, x_n]^T$, and $\mathbf{V} = [v_1, v_2, \dots, v_n]^T$. Equation (1) can be expressed as:

$$\begin{cases} \dot{\mathbf{X}} = \mathbf{V} \\ \dot{\mathbf{V}} = \mathbf{G}(\mathbf{U}' + \mathbf{D}) \end{cases} \quad (4)$$

where $\mathbf{G} = \text{diag}[m_1, m_2, \dots, m_n]^{-1}$, $\mathbf{U}' = [u'_1, u'_2, \dots, u'_n]^T$, $\mathbf{D} = [d_1, d_2, \dots, d_n]^T$, in which d_i refers to the composite disturbance term and is given by $d_i = f_{i-1} - f_{di} - f_i$.

Remark 1: During the operation of the high-speed train, the unknown composite disturbance d_i includes the running resistance f_{di} and the two interactive forces f_{i-1} and f_i acting on the i_{th} carriage. While the train is braking, the running resistance f_{di} is bounded, as v_i is measurable; If no fracture exists at the connection between carriages during the braking, then Δx_i and Δv_i are bounded. Therefore, f_{i-1} and f_i are also bounded. In summary, the composite disturbance d_i is a bounded unknown, and the elements in vector $\mathbf{D} = [d_1, d_2, \dots, d_n]^T$ are bounded unknowns, that is, $|d_{\max}| \leq \lambda$, where λ is a positive constant.

III. DESIGN AND STABILITY OF THE SLIDING MODE CONTROLLER

The given value of the braking force of each carriage when the train runs stably is calculated using the designed controller. For the whole train, the cumulative sum of the output values of each controller can be used as the longitudinal target braking force, and the stability of the controller is proved at the same time. Tracking error is defined as:

$$\mathbf{e} = [e_1, e_2, \dots, e_n]^T \text{ and } \dot{\mathbf{e}} = [\dot{e}_1, \dot{e}_2, \dots, \dot{e}_n]^T$$

where $e_i = x_i - x_d$ and $\dot{e}_i = \dot{x}_i - \dot{x}_d$, in which x_d refers to the given reference curve when braking, which is n -order differentiable.

The sliding surface is designed as:

$$\mathbf{s} = \mathbf{c}\mathbf{e} + \dot{\mathbf{e}} \quad (5)$$

where $\mathbf{c} = \text{diag}[c_1, c_2, \dots, c_n]$, $c_i > 0$, and $\mathbf{s} = [s_1, s_2, \dots, s_n]^T$.

Then:

$$\dot{\mathbf{s}} = \mathbf{c}\dot{\mathbf{e}} + \ddot{\mathbf{e}} = \mathbf{c}\dot{\mathbf{e}} + \mathbf{G}(\mathbf{U}' + \mathbf{D}) - \ddot{\mathbf{X}}_d \quad (6)$$

where $\dot{\mathbf{s}} = [\dot{s}_1, \dot{s}_2, \dots, \dot{s}_n]^T$, $\mathbf{X}_d = [x_d, \dot{x}_d, \dots, x_d]^T$.

Theorem 1. The sliding mode controller (7) is designed for the high-speed train system model (4). The displacement error of the system $\|\mathbf{e}\|$ is gradually approaching to zero, the controller is:

$$\mathbf{U}' = \mathbf{M}[-\mathbf{c}\dot{\mathbf{e}} + \ddot{\mathbf{X}}_d - \mathbf{\Gamma}\mathbf{S}_d] \quad (7)$$

where $\mathbf{M} = \text{diag}[m_1, m_2, \dots, m_n]$, $\mathbf{S}_d = [\text{sgn}(s_1), \text{sgn}(s_2), \dots, \text{sgn}(s_n)]^T$, and $\mathbf{\Gamma} = \text{diag}[\eta_1, \eta_2, \dots, \eta_n]$, η_i is a constant greater than zero.

Proof: The Lyapunov function is defined as:

$$V = \frac{1}{2} \mathbf{s}^T \mathbf{s} \quad (8)$$

By taking the first-order derivative of equation (8) with respect to time, the following equation can be obtained:

$$\begin{aligned} \dot{V} &= \mathbf{s}^T \dot{\mathbf{s}} \\ &= \mathbf{s}^T \{ \mathbf{c}\dot{\mathbf{e}} + (-\mathbf{c}\dot{\mathbf{e}} + \ddot{\mathbf{X}}_d - \mathbf{\Gamma}\mathbf{S}_d) + \mathbf{G}\mathbf{D} - \ddot{\mathbf{X}}_d \} \\ &= \mathbf{s}^T (-\mathbf{\Gamma}\mathbf{S}_d + \mathbf{G}\mathbf{D}) \\ &\leq -\eta_{\min} \|\mathbf{s}\|_1 + \frac{1}{m_i} d_{\max} \|\mathbf{s}\|_1 \\ &= -\|\mathbf{s}\|_1 \left(\eta_{\min} - \frac{1}{m_i} d_{\max} \right) \end{aligned} \quad (9)$$

By taking $\eta_{\min} \geq \frac{\lambda}{m_i} + \sigma$ ($\sigma > 0$), then:

$$\dot{V} \leq -\|\mathbf{s}\|_1 \sigma \quad (10)$$

Thus, the system satisfies the condition of reaching the sliding surface. Thereafter, the following equation can be obtained according to equivalence theory [16]:

$$s = \dot{s} = 0 \tag{11}$$

As shown in formula (5), the displacement error and velocity error of the system during the braking process gradually approach zero, that is:

$$\lim_{t \rightarrow \infty} \|e\| = 0 \text{ and } \lim_{t \rightarrow \infty} \|\dot{e}\| = 0$$

Note 1: The scope of the braking force is distributed in the whole train in this study. When a wheelset of a train slides, the braking force of the wheelset decreases, which leads to the loss of the total braking force of the train. The total braking force should remain unchanged to ensure good braking performance and low energy consumption. Here, the target braking force is given by:

$$F = -(u'_1 + u'_2 + \dots + u'_n) \tag{12}$$

where F refers to the total target braking force.

IV. OPTIMAL DISTRIBUTION OF BRAKING FORCE

An optimal distribution algorithm is designed for the braking force based on the established objective function and the selected constraint conditions. The braking force after optimized distribution in each carriage is obtained by solving the optimization problems satisfying the abovementioned model, the objective function, and the train operation constraints.

4.1 Establishment of the objective function

An important parameter for describing the braking capacity of a train is the adhesion utilization ratio, which represents the ratio of the adhesive strength used in practice to the maximum adhesive strength that can be achieved by means of the design between the wheel and the rail [17]:

$$\beta = \frac{N}{\mu P} (0 \leq \beta \leq 1) \tag{13}$$

where N refers to the adhesive strength used in practice; μ is an adhesion coefficient; and P is adhesive gravity. The longitudinal force analysis shows that the adhesive strength used in the braking process is the braking force exerted by the train.

The adhesion coefficient on the wet rail surface is given by [18]:

$$\mu = \partial_1 + \frac{\partial_2}{v + \partial_3} \tag{14}$$

where v refers to the velocity of the train (km/h), with $\partial_1 = 0.0405$, $\partial_2 = 13.55$, and $\partial_3 = 120$.

In the braking process, the train is required to exert great braking force within the range of adhesion to ensure that it can stop as quickly as possible, that is, β is maximum and $(1-\beta)^2$ is minimum. Then, the problem on force distribution is transformed into a problem of finding the optimal solution. The objective function is constructed as follows:

$$\min f = W_1 \left(1 - \frac{u_1}{\mu_1 P_1}\right)^2 + W_2 \left(1 - \frac{u_2}{\mu_2 P_2}\right)^2 + \dots + W_n \left(1 - \frac{u_n}{\mu_n P_n}\right)^2 \tag{15}$$

where W_i refers to the weighting factor, and $0 < W_i < 1$; u_i refers to the braking force to be distributed in operation in the i_{th} carriage of high-speed train; and $\mu_i P_i$ refers to the maximum adhesive strength that the i_{th} carriage can provide.

Lemma 1 [19]: Sufficient conditions for the existence of extremum of multivariate function: Hessian matrix \mathbf{H} is a positive definite, get the minimum value; Hessian matrix \mathbf{H} is a negative definite, get the maximum value.

The existence of the minimum value of the objective function is proven in the next part. Let:

$$b_i = \frac{1}{\mu_i P_i} \tag{16}$$

Then, the objective function equation (15) is transformed into:

$$\min f = W_1 (1 - b_1 u_1)^2 + W_2 (1 - b_2 u_2)^2 + \dots + W_n (1 - b_n u_n)^2 \tag{17}$$

Hessian matrix \mathbf{H} is calculated as:

$$\mathbf{H} = \begin{bmatrix} \frac{\partial^2 f}{\partial u_1^2} & \frac{\partial^2 f}{\partial u_1 \partial u_2} & \dots & \frac{\partial^2 f}{\partial u_1 \partial u_n} \\ \frac{\partial^2 f}{\partial u_2 \partial u_1} & \frac{\partial^2 f}{\partial u_2^2} & \dots & \frac{\partial^2 f}{\partial u_2 \partial u_n} \\ \vdots & \vdots & \ddots & \vdots \\ \frac{\partial^2 f}{\partial u_n \partial u_1} & \frac{\partial^2 f}{\partial u_n \partial u_2} & \dots & \frac{\partial^2 f}{\partial u_n^2} \end{bmatrix} \quad (18)$$

By calculating the second partial derivative of objective function equation (17), the following equation can be obtained:

$$\begin{aligned} \frac{\partial^2 f}{\partial u_1^2} &= 2W_1 b_1^2, \dots, \frac{\partial^2 f}{\partial u_n^2} = 2W_n b_n^2 \\ \frac{\partial^2 f}{\partial u_i \partial u_j} &= 0 (i \neq j) \end{aligned} \quad (19)$$

From equations (18) and (19), Hessian matrix \mathbf{H} of objective function can be obtained as:

$$\mathbf{H} = \begin{bmatrix} 2W_1 b_1^2 & 0 & \dots & 0 \\ 0 & 2W_2 b_2^2 & \dots & 0 \\ \vdots & 0 & \ddots & 0 \\ 0 & 0 & \dots & 2W_n b_n^2 \end{bmatrix} \quad (20)$$

Obviously, \mathbf{H} is a positive-definite matrix. **Lemma 1** can be used to prove the existence of the minimum value in the constructed objective function.

4.2 Selection of constraint conditions

The braking process of a high-speed train is restricted by many factors. The adhesion restriction can endanger the train's operation safety. The ride comfort of passengers can also be used to measure the stability of the high-speed train. Therefore, adhesion restriction and ride comfort are both considered together with the selected constraint conditions in this study:

$$s.t. \begin{cases} u_1 + u_2 + \dots + u_n = F \\ 0 \leq u_i \leq \mu_i P_i \end{cases} \quad (21)$$

And,

$$s.t. \begin{cases} m_1 a_1 + f_1 + f_{d1} \leq u_1 \leq m_1 a_2 + f_1 + f_{d1}, i = 1 \\ m_i a_1 + f_i - f_{i-1} + f_{di} \leq u_i \leq m_i a_2 + f_i - f_{i-1} + f_{di}, i = 2, 3, \dots, n-1 \\ m_n a_1 - f_{n-1} + f_{dn} \leq u_n \leq m_n a_2 - f_{n-1} + f_{dn}, i = n \end{cases} \quad (22)$$

where $f_0 = 0$ and $f_n = 0$. $a_1 = 0.981m/s^2$, $a_2 = 1.1772m/s^2$ [20].

Note 2: Equations (21) and (22) consist of three parts. In the first part, the equality constraint indicates that the total target braking force F remains constant in the braking process. In the second part, the inequality constraint indicates that the braking force after optimized distribution u_i in each carriage cannot exceed the maximum adhesion restriction $\mu_i P_i$ between the wheel and rail; otherwise, it will cause train sliding. The third part corresponds to the constraint condition of ride comfort. In general, the acceleration of ride comfort is in the range of $a_1 - a_2$. The braking force is limited by the restricted acceleration.

4.3 Solutions

On the basis of the characteristics of the proposed objective function and constraint conditions, the problems should be transformed into quadratic programming form to be able to obtain the abovementioned variables [21]. By solving the optimal solution in the form of quadratic programming, the braking force after optimized distribution in each carriage can be further obtained [22]. Here, the equivalent transformation is conducted for the objective function equation (17) and constraint equations (21) and (22) constructed in this study.

In the following part, let:

$$Z_i = 1 - b_i u_i \quad (23)$$

Then, the objective function equation (17) can be transformed into:

$$\begin{aligned} \min f &= W_1 Z_1^2 + W_2 Z_2^2 + \dots + W_n Z_n^2 \\ &= \frac{1}{2} (Z_1 \quad Z_2 \quad \dots \quad Z_n) \begin{pmatrix} 2W_1 & 0 & \dots & 0 \\ 0 & 2W_2 & 0 & 0 \\ \vdots & 0 & \ddots & \vdots \\ 0 & 0 & \dots & 2W_n \end{pmatrix} \begin{pmatrix} Z_1 \\ Z_2 \\ \vdots \\ Z_n \end{pmatrix} \end{aligned} \quad (24)$$

Subsequently, the constraint equations (21) and (22) can be transformed into :

$$\text{s.t.} \begin{cases} \frac{1}{b_1} Z_1 + \frac{1}{b_2} Z_2 + \dots + \frac{1}{b_n} Z_n = \left(\frac{1}{b_1} + \frac{1}{b_2} + \dots + \frac{1}{b_n} \right) - F \\ 0 \leq Z_i \leq 1 \end{cases} \quad (25)$$

And,

$$\text{s.t.} \begin{cases} 1 - b_1(m_i a_2 + f_1 + f_{d1}) \leq Z_1 \leq 1 - b_1(m_1 a_1 + f_1 + f_{d1}) & i=1 \\ 1 - b_i(m_i a_2 + f_i - f_{i-1} + f_{di}) \leq Z_i \leq 1 - b_i(m_i a_1 + f_i - f_{i-1} + f_{di}) & i=2,3,\dots,n-1 \\ 1 - b_n(m_n a_2 - f_{n-1} + f_{dn}) \leq Z_n \leq 1 - b_n(m_n a_1 - f_{n-1} + f_{dn}) & i=n \end{cases} \quad (26)$$

let $\xi_i = m_i a_2 - f_{i-1} + f_{di} + f_i = 94176 - d_i$ and $\zeta_i = m_i a_1 - f_{i-1} + f_{di} + f_i = 78480 - d_i$

Equation (26) can then be simplified as:

$$1 - b_i \xi_i \leq Z_i \leq 1 - b_i \zeta_i \quad (27)$$

Constraint equations (25) and (27) can be combined into:

$$\text{s.t.} \begin{cases} 0 \leq Z_i \leq 1 \\ \frac{1}{b_1} Z_1 + \frac{1}{b_2} Z_2 + \dots + \frac{1}{b_n} Z_n = \left(\frac{1}{b_1} + \frac{1}{b_2} + \dots + \frac{1}{b_n} \right) - F \\ 1 - b_i \xi_i \leq Z_i \leq 1 - b_i \zeta_i \end{cases} \quad (28)$$

For the abovementioned quadratic programming, *Simulink* is used to construct the model [23], and a program is written to obtain the optimal solution Z_i . Then, u_i is obtained by substitution:

$$u_i = \frac{1 - Z_i}{b_i} \quad (29)$$

Note 3: The force u_i calculated in this study does not distinguish the electric braking force and air braking force. The focus is on the specific analysis of the distribution of braking force in each carriage during operation control. Therefore, u_i only acts as a joint force on the carriages of the high-speed train.

The braking force optimization distribution control structure of a high-speed train is shown in **Fig. 2**.

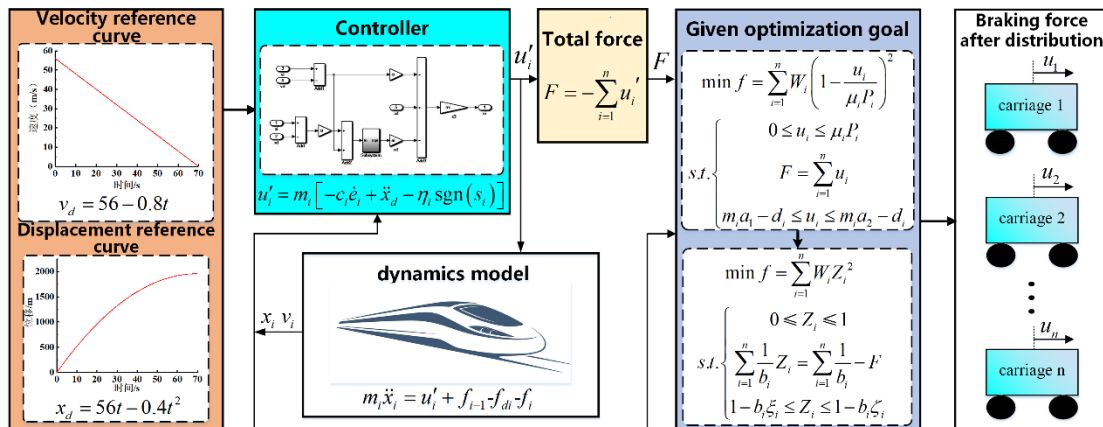


Fig. 2: Diagram of the braking force optimization distribution control structure of a high-speed train

V. SIMULATION VERIFICATION

A simulation experiment is performed to explore the effect of the abovementioned optimization algorithm. As a means of facilitating the simulation, only four carriages are used for the high-speed train to verify the effectiveness and feasibility of the proposed algorithm. The parameters of the operation dynamic model of the high-speed train are shown in **Table 1**.

Table 1 Model parameters of the carriages of the high-speed

Parameters	Value	Unit
m_1, m_2, m_3, m_4	80000	kg
φ_1	1.176×10^{-2}	N / kg
φ_2	7.7616×10^{-4}	Ns / mkg
φ_3	1.6×10^{-5}	Ns ² / m ² kg
k	80000	N / m
h	40000	kg / s

The given braking reference curve in the braking process is a curve with an initial velocity of $56m/s$ and a deceleration of $0.8m/s^2$. The simulation parameter values are set to $c_i = 1$, $\eta_i = 30$.

The adhesion coefficient used in this study is simply related to velocity, but the adhesion between the wheel and rail is an extremely complicated tribological process. The adhesion restriction of the head carriage is generally at the minimum, indicating that this carriage bears the minimum weight. After the head carriage run, the rail surface is cleaned. Therefore, the adhesion restriction of the succeeding carriages is increased. However, the adhesion restriction of the tail carriage is minor. This is because the rail may absorb impurities during operation. So the third carriage has the most weight, and the second carriage has the second highest weight. The weight of each carriage of the high-speed train as determined in this study is shown in **Table 2**.

Table 2 Weight of each carriage of high-speed train

weight	W_1	W_2	W_3	W_4
Value	0.1	0.3	0.4	0.2

5.1 Simulation of tracking control

By designing the controller, each carriage can track the given braking reference curve, and the target braking force can be obtained. **Fig. 3** shows the three-dimensional response curve of the speed and displacement of each carriage to track the desired trajectory of the train, whereas **Figs. 4** and **Figs. 5** show the corresponding error curves of each carriage to track the desired trajectory of the train. The displacement error of each carriage converges to zero within 5 s (**Fig. 4**).

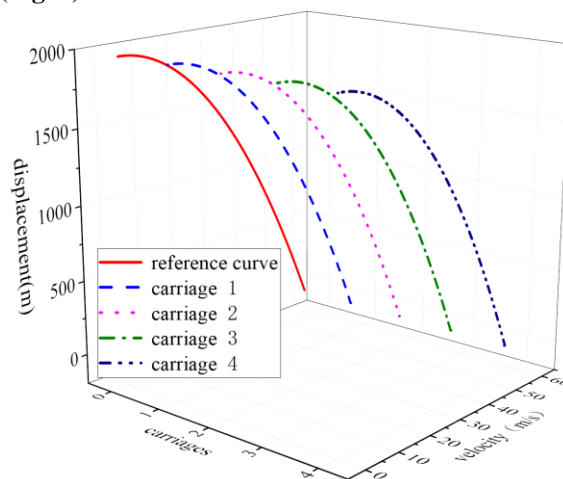


Fig. 3: Velocity–displacement diagram

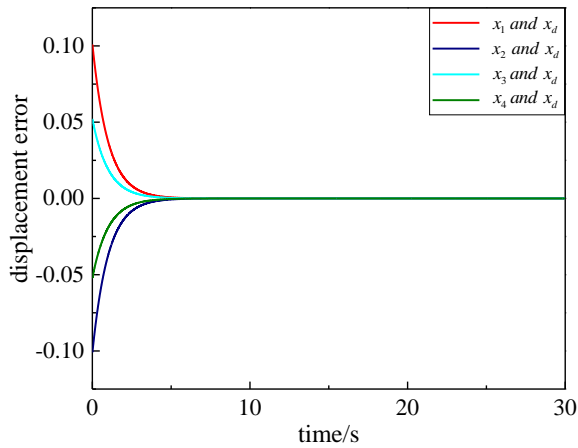


Fig. 4: Displacement error diagram

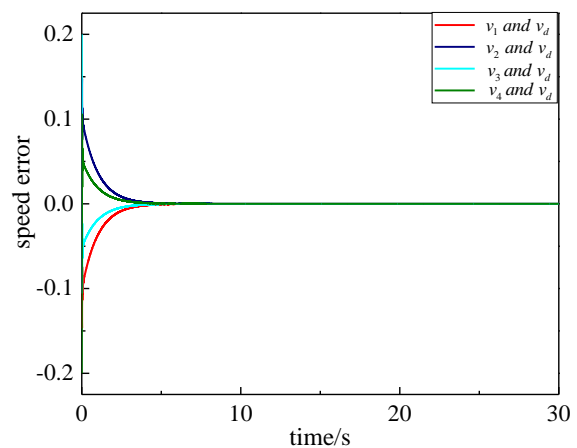


Fig. 5: Velocity error diagram

5.2 Simulation of braking force distribution

The braking distribution before optimization is the distribution that does not consider any constraint condition, which can also be regarded the average distribution. However, in view of avoiding high-speed train sliding, the braking force should be distributed on the basis of the weight of each carriage in the practical braking process. Here, the adhesion restriction in each carriage and ride comfort are both considered.

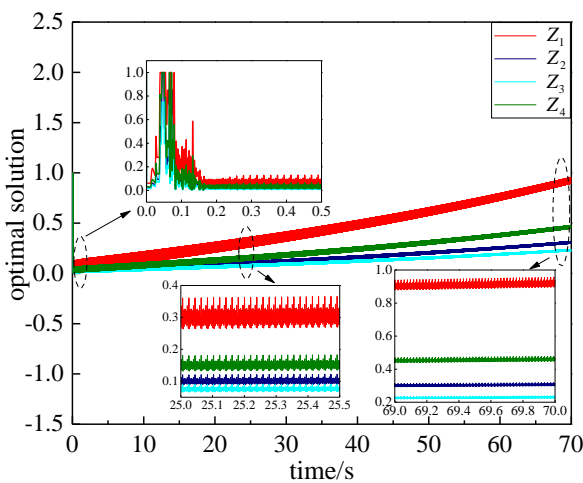


Fig. 6: Optimal solution

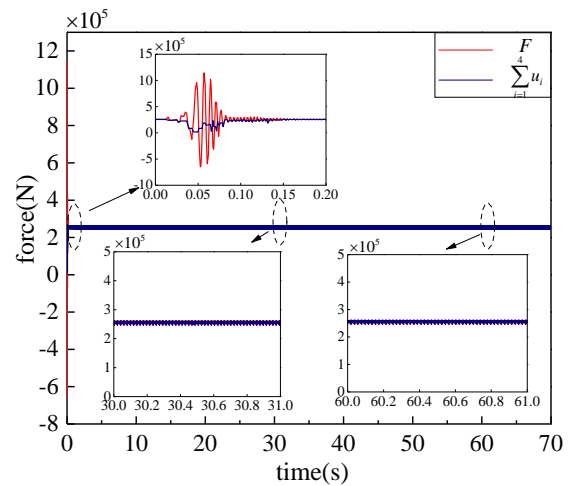


Fig. 7: Equality constraint

Fig. 6 shows the change curve of the optimal solution of each carriage. The optimal solution continuously increases as the velocity and adhesion utilization rate gradually decrease during the braking process. When the braking is 70 s, the velocity decreases to 0m/s, whereas the optimal solution increases to 1. Fig. 7 shows the equality constraint. After the total target braking force before and after optimization is kept the same within 0.15s, the cumulative sum of the braking force distributed in each carriage remains equal to the total target braking force in the subsequent distribution process. The trend proves that the equality constraint is true.

From the transformation relationship between optimal solution and braking force, the braking force distributed after optimization can then be obtained. Figs. 8–11 show a comparison of the braking force before and after optimization in four carriages. As the weight of the first carriage is the smallest, the braking force distributed in the first carriage after optimization is less than that before optimization (Fig. 8). Then, as the velocity continues to decrease, the adhesion restriction continues to increase. In the range of 0–0.15 s, the braking force exerted before optimization is greater than the adhesion restriction, which causes the train to slide. As for the whole braking process, the braking force distributed after optimization is maintained within the scope of adhesion restriction.

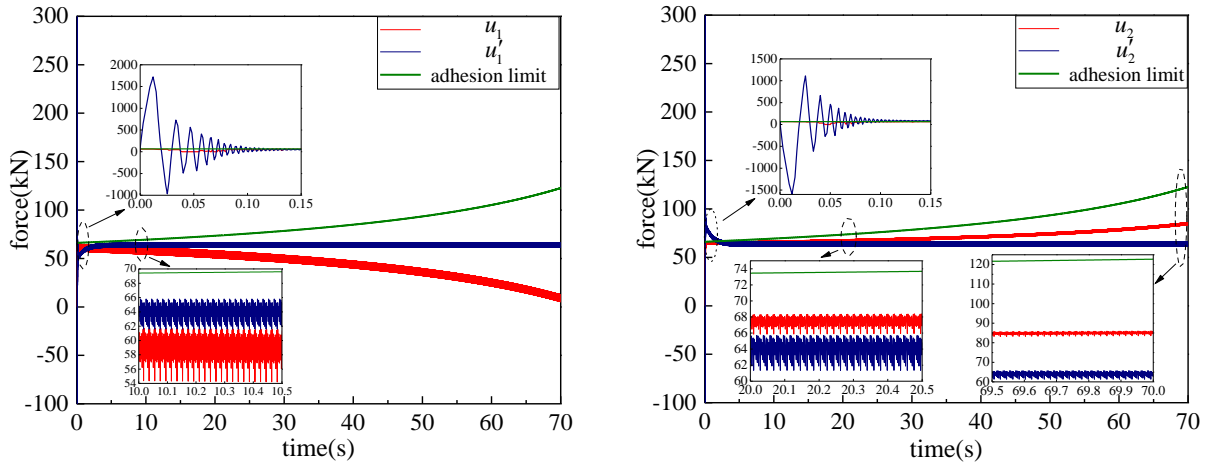


Fig. 8-9: Comparison of braking force of carriages 1 and 2 before and after optimization

Figs. 9 and Figs. 10 show that the braking forces distributed in carriages 2 and 3 after optimization increases with the increase in adhesion restriction. Carriage 3 has the largest weight in the whole train, thus, the braking forces distributed after optimization increases the most. However, the braking forces distributed in the two carriages after optimization still do not exceed respective adhesion restriction. Fig. 11 shows that no significant difference exists in the braking force distributed in carriage 4 before and after the optimization. This finding can be attributed to the minimal difference in the weight of carriage 4 before and after the optimization.

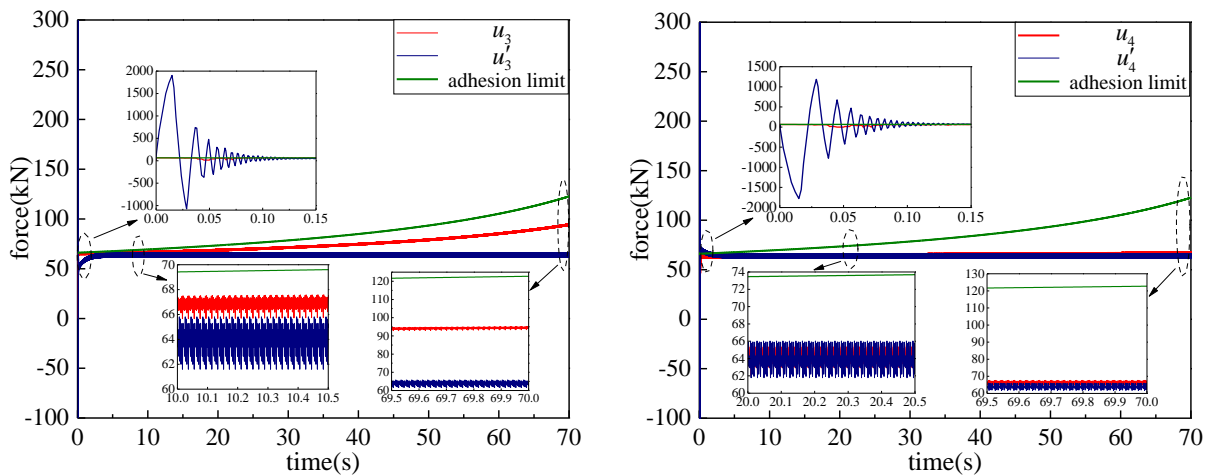


Fig. 10-11: Comparison of braking force of carriages 3 and 4 before and after optimization

In summary, in contrast to the braking force distributed before optimization, the braking force distributed after optimization varies according to the different weights of the carriages in the whole train. The optimal distribution method can ensure both the adhesion restriction and the ride comfort of passengers.

VI. CONCLUSIONS

This study calculates the longitudinal target braking force of a high-speed train based on its dynamic model. The dynamic simulation model of the train is constructed in *Matlab / Simulink*. Under the premise of a given target braking force, the objective optimized function by using adhesion utilization rate is established. Then, the optimal distribution algorithm of braking force is studied by fully considering the adhesion restriction and ride comfort of passengers. The simulation results indicate that the braking force optimization distribution method proposed in this study offers significant advantages with respect to the average distribution method. The braking force distributed in each carriage after optimization varies according to the different weights of carriages, further indicating that it can meet the requirements of practical working conditions and achieve the preset distribution logic.

ACKNOWLEDGMENTS

This research was supported by the Natural Science Foundation of China (nos. U1934219, 61773159), Excellent Youth Research Project of Education Department of Hunan Province (nos. 18B303), Project of Hunan Provincial Department of Education (nos. 19A137), and Hunan Provincial Natural Science Foundation of China (nos. 2020JJ6083).

REFERENCES

- [1]. Xiaochun Fang, Shuai Lin, Zhongping Yang, et al. Adhesion Control Strategy Based on the Wheel-Rail Adhesion State Observation for High-Speed Trains. *Electronics*, 7(5), 2018, 70.
- [2]. Kun Xu, Jing Zeng and Lai Wei. An analysis of the self-excited torsional vibration of high-speed train drive system. *Journal of Mechanical Science and Technology*, 33(3), 2019, 1149-1158.
- [3]. Alejandro Bustos, Higinio Rubio, Cristina Castejón, et al. EMD-Based Methodology for the Identification of a High-Speed Train Running in a Gear Operating State. *Sensors*, 18(3), 2018, 793.
- [4]. Zhang Changfan, Yin Xiaofei, He Jing, et al. Research on optimized control of braking force redistribution. 2017 IEEE 13th International Conference on Electronic Measurement & Instruments (ICEMI), IEEE, 2017.
- [5]. Zhu Qinyue, Bao Shijiong, Tan Xitang, et al. Research on Optimization of Electro-pneumatic Braking Cooperative Control for EMU. *Computer Engineering*, 39(12), 2013, 17-21.
- [6]. Li Qi, Shang Weilin, Yan Yu, et al. Research on Braking Distribution and Braking Energy Recovery for Novel Power Supply Model Tram. *Proceedings of the CSEE*, 40(7), 2020, 2285-2294.
- [7]. Ma Zhengwei, Sun Daxu. Energy Recovery Strategy Based on Ideal Braking Force Distribution for Regenerative Braking System of a Four-Wheel Drive Electric Vehicle. *IEEE Access*, 2020(8), 2020, 136234-136242.
- [8]. Zhu Yueying, Wu Hao, Zhang Junxia. Regenerative Braking Control Strategy for Electric Vehicles Based on Optimization of Switched Reluctance Generator Drive System. *IEEE Access*, 2020(8), 2020, 76671-76682.
- [9]. He Jing, Shi Laicheng, Zhang Changfan, et al. Research on Electro-pneumatic Braking Force Optimization Distribution for Electric Multiple Unit. *Computer Engineering*, 44(10), 2018, 314-320.
- [10]. Wu Jun, Qiu Yi. Analysis of ride comfort of high-speed train based on a train-seat-human model in the vertical direction. *Vehicle system dynamics*, 2020, 1-27.
- [11]. Ma Huiru, Chen Dewang, Yin Jiateng. Riding Comfort Evaluation Based on Longitudinal Acceleration for Urban Rail Transit—Mathematical Models and Experiments in Beijing Subway. *Sustainability*, 12(11), 2020, 4541.
- [12]. González D, Milanés V, Pérez J, et al. Speed Profile Generation based on Quintic Bézier Curves for Enhanced Passenger Comfort. 2016 IEEE 19th International Conference on Intelligent Transportation Systems(ITSC). IEEE, 2016, 814-819.
- [13]. He Jing, Yang Buchong, Zhang Changfan, et al. Integrated cooperative braking algorithm of non-linear EMU with external disturbance. *The Journal of Engineering*, 2019(23), 2019, 8937-8941.
- [14]. He Jing, Yang Buchong, Zhang Changfan, et al. Robust consensus braking algorithm for distributed EMUs with uncertainties. *IET Control Theory and Applications*, 13(17), 2019, 2766-2774.
- [15]. Zhiwei Wang, Guiming Mei, Qing Xiong, Zhonghui Yin, et al. Motor car-track spatial coupled dynamics model of a high-speed train with traction transmission systems. *Mechanism and Machine Theory*, 137, 2019, 386-403.
- [16]. Liu Qi, Li Rongchang, Zhang Qingling, et al. Adaptive Robust H_∞ Sliding Mode Control for Singular Systems with Time-varying Delay and Uncertain Derivative Matrix. *International Journal of Control, Automation and Systems*, 17(12), 2019, 3179-3193.
- [17]. Rufeï Hou, Li Zhai, Tianmin Sun, Yuhua Hou, et al. Steering Stability Control of a Four In-Wheel Motor Drive Electric Vehicle on a Road with Varying Adhesion Coefficient. *IEEE Access*, 2019(7), 2019, 32617-32627.
- [18]. Spiroiu M A. About the influence of wheel-rail adhesion on the maximum speed of trains. *MATEC Web of Conferences*. EDP Sciences, 178, 2018, 06004.
- [19]. Sharipov, R.A., Multiple Discriminants and Extreme Values of Polynomials in Several Variables. *Journal of Mathematical Sciences*, 245(1), 2020, 89-97.
- [20]. Wang Haijun, Zeng Jing, Luo Guangbing, et al. Research on Adhesion and Non-Adhesion Braking Characteristics for High-Speed Train. *Applied Mechanics and Materials*, 121-126, 2011, 3437-3443.
- [21]. Bonami P, Günlük O, Linderoth J. Globally solving nonconvex quadratic programming problems with box constraints via integer programming methods. *Mathematical Programming Computation*, 10(3), 2018, 333-382.
- [22]. Manjunatha S C, Dr.Shankarappa F Kodad. To Dampen the Low Frequency Oscillations in the Power System Using the Supplementary Controller Design For the IPFC. *International Journal of Engineering Science Invention (IJESI)*, 9(11), 2020, 46-52.
- [23]. MarylinMartinez Baquero, Javier Martinez Baquero, et al. Design of Control Systemfor DC motor. *International Journal of Engineering Science Invention (IJESI)*, 9(9), 2020, 01-09.

Jing He, et. al. "Study on Brake Control for High-Speed Train Based on Optimal Distribution of Braking Force." *International Journal of Engineering Science Invention (IJESI)*, Vol. 10(02), 2021, PP 21-30.
Journal DOI- 10.35629/6734